EEG montage analysis in the Blind Source Separation framework

Ricardo A. Salido Ruiz[1], Radu Ranta[1], Valerie Louis-Dorr[1]

Centre de Recherche en Automatique de Nancy, UMR 7039 - Nancy-Université, CNRS 2, avenue de la forêt de Haye, 54516 Vandoeuvre, France. (e-mail: Ricardo-Antonio.Salido-Ruiz@ensem.inpl-nancy.fr., Radu.Ranta@ensem.inpl-nancy.fr., Valerie.Louis@ensem.inpl-nancy.fr

Abstract

Blind source separation (BSS) is a relatively recent technique, more and more applied in electroencephalographic (EEG) signal processing. Still, the classical mixing model of the BSS does not take into account the real recording set-up. In fact, a major problem in electrophysiological recording systems (*e.g.* ECG, EEG, EMG) is to find a region in the human body whose bio-potential activity can be considered as neutral as possible *i.e.*, a quasi-inactive reference place. Nowadays, it is well known that it is impossible to find a "zero-potential" site on the human body. In particular, the most common way of performing EEG recordings is by using as a common reference an electrode placed somewhere on the head. Starting from this Common Reference Montage (CRM), several other montages can be constructed to obtain alternative interpretation or processing solutions. Regardless of the chosen montage, the reference electrode intervenes in the mixing model of the BSS. The objective of this work is to analyse the influence of the montage on the mixing matrix and the quality of the BSS solution. This paper proposes to formalize the source separation problem in a non zero-potential

Preprint submitted to Biomedical Signal Processing and Control *May 5, 2010*

reference context and shows that the Average Reference Montage (ARM), augmented by a virtual "average measure", leads to better source separation results (separability index *IS*). This conclusion is supported by simulated EEGs using the most common montages *i.e.*, Common Reference Montage, Average Reference Montage and Bipolar-Longitudinal Montage, as well as by real EEG examples.
Keywords:
Reference electrode, EEG Montages, Blind Source Separation, Separability Index, Correlation Coefficient

1. Introduction

An important issue for the actual standard systems for bio-potentials recording (electrophysiological activity measuring systems as Electrocardiogram (ECG), Electroencephalogram (EEG), Electromyogram (EMG)) is to find a region in the human body whose bio-potential activity could be considered as neutral as possible. That is desirable because the electrical activity at that place affects measurements at all other active electrode sites, see [1] and [2].

In EEG, one of the most common recording systems is the 10-20 system of electrode placement. EEG recordings are performed by using electrodes placed at standardized locations on the head. These *measuring electrodes* are referenced either to cephalic or non-cephalic *reference electrodes*. This paper focuses on the most frequently employed cephalic reference. The anatomical landmarks most frequently used as cephalic references sites are the nasion, the inion, over the occipital area, the pre-auricular points, etc [3]. All these reference sites contribute with some non-desirable effects and perturbations on the recordings.

The previously described recording set-up is known as Common Reference Montage (CRM, cephalic) and it is the basis montage in acquisition systems. Nevertheless, to ease interpretation and processing in the absence of a zero-potential reference, several multiple combinations of differential measures have been derived from the CRM by some simple manipulations. The most common of these montages are the Average Reference Montage (ARM) and the Bipolar-Longitudinal Montage (BLM), see [4].

Regardless of the employed montage, all measured EEG signals can be seen as a result of an unknown mixture of several unknown cortical sources, extra-cortical artefacts and noise. A relatively recent signal processing technique, the Blind Source Separation (BSS), can be used to separate these mixed measured signals in "independent" sources, which can be further-on used, in a pre-processing context, either for artefact elimination or for brain activity evaluation, [5–9]. The classical BSS model supposes ideally measured signals, *i.e.*, zero-referenced, while real electrophysiological recordings have a non-null reference. Most of the EEG literature concerning BSS methods does not take into account this problem. A solution proposed by [10] consists in identifying the reference signal by constraining the BSS model to particular mixing system which implies that the non-zero reference signal is independent from all other measures. In the recording set-up used by the authors (intra-cranial measures), this approach is based on the hypothesis that the reference electrode placed on the scalp is not influenced by the intracranial measures.

If for intra-cranial measures this hypothesis (although not proven) can be employed, in a cephalic referenced scalp EEG (CRM) context it cannot hold, as the reference electrode itself records a noisy mixture of cerebral and extra-cerebral sources. Therefore it is important to evaluate the quality of the obtained separation function of the measured signals, *i.e.*, from the employed montage. One could object that all the different montages can be obtained by linear transformation from the CRM and therefore the source separation solution should be the same independently of the montage. Still, the noise affects them differently, and the solutions are not identical, as it is shown in section 3 and illustrated by simulation and by real examples in section 4. In particular, it is proven that the ARM, augmented by a "virtual measure" consisting in the actual average of the CRM signals, performs better than CRM or BLM and that it tends asymptotically towards an ideal zero-referenced montage (ZRM), and therefore should be used when source separation algorithms are applied.

In this work we propose the following approach in order to evaluate the influence of the EEG montage in the BSS and a noisy framework. In the second section we present an introduction to the BSS problem extended to the noisy case which is a more realistic model, followed by a brief description of some BSS algorithms commonly mentioned in the literature and evaluated in this paper (SOBI-RO, SOBI, and FastICA). The employed performance criteria are introduced in the last part of the second section, both for simulated and real EEGs. In the third section we propose a model for the EEG montages presented in this work, emphasising the influence of noise, which is different for the different montages and thus influences the quality of the

BSS estimations. In the fourth section we present the results along with a discussion about the most remarkable interpretations. The paper ends with the conclusion and perspective section.

2. Source Separation

The final objective of blind source separation is to recover all the independent sources from the observed EEG recordings. In general, these observations are modeled as a linear mixture of independent sources, both the mixing system and the sources being unknown.

2.1. Classical BSS Model

The classical linear mixing model can be written, at each instant k, as:

$$\mathbf{x} = \mathbf{A}\mathbf{s}. \tag{1}$$

where $\mathbf{x}$ is a vector of M observed signals (EEG channels), $\mathbf{A}$ is the unknown full-column rank mixing matrix ($M \times N$) and $\mathbf{s}$ is the vector of N independent unknown sources (we consider here only the case $M \geq N$, that is, we have more sensors than sources and the separation problem has a solution). In order to estimate the original sources it is necessary to calculate the following linear transformation:

$$\mathbf{y} = \mathbf{W}\mathbf{x} = \mathbf{W}\mathbf{A}\mathbf{s}. \tag{2}$$

where $\mathbf{y}$ is a vector of N estimated sources and $\mathbf{W}$ is the $(N \times M)$ linear transformation that allows separating the mixed signals in their independent components. Theoretically, such transformation $\mathbf{W}$ should be the (left pseudo) inverse of the mixing matrix $\mathbf{A}$, when sources are perfectly recovered. When $M > N$, the obtained mixture is redundant and the number of sources really present in the mixture (and thus the dimensions of $\mathbf{W}$) must be estimated by the separation algorithm. The most currently employed solution is to evaluate the number of linearly independent measures in the mixture (which in fact is equal to the number of sources estimated by the BSS algorithms) by using some criterion based on the eigen-values of the covariance matrix of the measured signals (Akaike Information Criterion AIC, Minimum Description Length MDL or Bayesian Information Criterion BIC, see [11] for details).

However, obtaining the exact inverse of the mixing matrix $\mathbf{A}$ is impossible to achieve, see for example [11]. Thus, source separation algorithms are focused in finding a matrix $\mathbf{W}$ such as $\mathbf{G} = \mathbf{WA}$ be a permuted and scaled diagonal matrix (one non-null value by line and column), which implies that the sources are recovered, excepting their order and their amplitude.

A more realistic model considers noisy measures and it can be written as follows:

$$\tilde{\mathbf{x}} = \mathbf{As} + \mathbf{n}. \tag{3}$$

where $\tilde{\mathbf{x}}$ is the noisy measure vector ($M \times 1$), $\mathbf{A}$ is the unknown full-column rank mixing matrix ($M \times N$, $\mathbf{s}$ is the sources vector ($N \times 1$) and $\mathbf{n}$ is a vector ($M \times 1$) of independent Gaussian noises. By BSS, one will find a separation matrix $\mathbf{W}$ and noisy source estimates $\tilde{\mathbf{y}}$.

2.2. BSS Algorithms

Several Blind Source Separation (BSS) algorithms have been proposed and analysed during the last decades. Most of them solve the BSS problem based on different hypothesis about the nature of the sources they are separating. Globally, source separation algorithms lay into two categories: those based on High Order Statistics (HOS) and those based on Second Order statistics (SOS). The HOS algorithms are well known as ICA algorithms, because the sources are assumed statistically independent. Consequently, the basic assumption of this family of algorithms is that the measured signals are a linear combination of unknown statistically independent zero mean sources. Because these algorithms are based on HOS such as kurtosis, they find the all the non-Gaussian independent sources. This is a restriction when the real sources are Gaussian, however if we are interested in extracting a particular source that we know is not Gaussian, this kind of algorithms are very efficient. One of the most popular and efficient algorithms from this family is the FastICA based on the fixed-point algorithm developed by A. Hyvärinen in [12], which is one of the fastest ICA algorithms. On the other hand, the family of SOS algorithms makes weaker assumptions about the statistical independence of the sources and they are capable of estimating Gaussian sources. In the SOS framework, the absence of the strong hypothesis of independence is compensated by other assumptions on the sources: (they must be either auto-correlated (*i.e.*, , non-white), non-stationary or both)Je change par: . Two of the most representative algorithms of this family are the Second Order Blind Identification (SOBI) and the Second Order Blind Identification with Robust Orthogonalization (SOBI-RO). SOBI was first introduced by A. Belouchrani [13] and it is an approach based on a joint diagonalization of several time-delayed covariance matrices. SOBI-RO [14] is an improvement of SOBI; the main differences between SOBI and SOBI-RO are the Robust Orthogonalization included in the pre-whitening step. The main advantages of these algorithms are their hypothesis are a priori verified for real EEG signals, which are band-limited and noisy.

These algorithms were already successfully applied for EEG separation, for example by [15] and [16] thus, we have included it into our analysis. However, it is not the objective of this of this work to explore the effectiveness of all these different methods, but to evaluate the impact of the employed montage. More details can be found in the cited references.

2.3. Performance Evaluation for Simulated EEG

The classical performance evaluation for source separation algorithms is based on the transfer matrix between original sources $\mathbf{s}$ and estimated ones $\tilde{\mathbf{y}}$, ($\mathbf{G} = \mathbf{WA}$).

The separability index IS is a distance measure between $\mathbf{G}$ and a diagonal permuted matrix and is computed by performing the following manipulations: the first step is to normalize the rows $\mathbf{g}_i$ of the matrix $\mathbf{G}$ by dividing each element by the maximum absolute value of the row:

$$\mathbf{g}_i^{'} = \frac{|\mathbf{g}_i|}{\max|\mathbf{g}_i|}. \tag{4}$$

From the normalized matrix $\mathbf{G}'$, the separability index is computed as follows:

$$IS = \frac{\sum_{j=1}^{N}(\sum_{i=1}^{N}(\mathbf{G}'(i,j)) - 1)}{N(N-1)}. \tag{5}$$

From (5) we can see that for a perfect separation the IS index is zero.

2.4. Performance Evaluation for Real EEG

In a real BSS context, applied on EEG recordings, we don't know the mixing matrix and the sources. Thus the classical performance evaluation based on the mixing matrix coefficients and presented for the simulated signal (equation 5) cannot be applied. However, under certain conditions, we can have information on particular electrophysiological sources like the ECG for example. If we are certain of the presences of this sources in the mixing (measured EEG) the BSS algorithm should be capable to find this signal as a source. Moreover, this source must present a great similarity with the ECG recorded simultaneously with the EEG. A high degree of similarity, measured for example using the cross-correlation, will indicate that the separation is effective, and thus can be used as an alternative performance criterion.

To take into account the ECG propagation time, we introduced a variable parameter of delay in the cross-correlation evaluation. In this way, the degree of similarity will be evaluated by taking the correlation between the recorded model signal (ECG) and the estimated source at the time lag of its maximum value.

Thus let $\mathbf{r}_{s_k,\hat{s}_k}$ be our performance criterion based on the correlation coefficient between the known source s_k and the estimated source $\hat{s}_k$ obtained by a time lag where it achieves the maximum value as follows:

$$\mathbf{r}_{s_k,\hat{s}_k} = \max_{\tau} \frac{cov(s_k(t), \hat{s}_k(t+\tau))}{\sigma_{s_k}\sigma_{\hat{s}_k}}, \qquad -a < \tau < a. \tag{6}$$

where a is a user chosen maximum time lag.

3. EEG montages models

In this section we propose to formalize the linear mixing model used in BSS in a non zero-potential reference context for cephalic reference. The newly derived models will allow a more precise definition of the different montages and of their influence on the performances of the BSS algorithms.

The previously proposed model (3) considers sensors $\tilde{\mathbf{x}}$ as measured relatively to an ideal null reference. However, in clinical implementation, it is not possible to measure relatively to a "zero-potential" electrode. In practice, one should consider "the measure" as the electrode pair made by the recording electrode and the reference electrode. Therefore, it is necessary to consider the way the measures are performed, *i.e.*, the recording set-up employed (CRM, ARM or BLM). In particular, when a cephalic reference is used, the reference electrode is not exempt from the influence of the same sources as the other measuring electrodes.

As mentioned in the introduction, the real acquisition montage is the CRM, which is derived from the recorded potentials of the sensors $\tilde{\mathbf{x}}$. Any other EEG montage (ARM, BLM) can be seen as a linear transformation of the CRM. In other words, the measures from the different montages are obtained as linear transformations of the recorded potentials $\tilde{\mathbf{x}}$, so also a noisy linear combination of sources $\mathbf{s}$. This suggests that the "montage" has no influence on the separation. However, as showed next, the noise has a different effect for the different montages and therefore the separation results are influenced by the chosen montage.

The following paragraphs propose to formalize the different montages in a source separation framework.

3.1. Common Reference Montage (CRM)

Consider a simple ideal model with N zero-referenced sources s_j, ($j = 1...N$) and M zero-referenced electrodes noisy $\tilde{x}_i$, $i = 1...M$ (eq. 3).

On the other hand, in a realistic noisy set-up, the common-referenced observations $\tilde{\mathbf{x}}_{CRM,i}$ (EEG signals) can be represented as:

$$\tilde{x}_{CRM,i} = \tilde{x}_i - \tilde{R}, \quad \text{with} \quad \tilde{R} = \tilde{x}_M, \quad i = 1...M-1. \tag{7}$$

where $\tilde{x}_{CRM,i}$ is a vector that contains the i-th cephalic-referenced electrode, $\tilde{x}_i$, is a hypothetical zero-referenced vector containing the noisy potentials recorded by the i-th sensor, $\tilde{R}$ is the reference vector associated to the cephalic reference electrode $\tilde{x}_M$. To separate the informative measures and the noise, equation (7) can be rewritten as:

$$\tilde{x}_{CRM,i} = x_i - x_M + (n_i - n_M) = x_{CRM,i} + n_{CRM,i} \tag{8}$$

In a source separation framework, the model for the real common reference montage becomes:

$$\tilde{\mathbf{x}}_{CRM} = \mathbf{A}_{CRM}\mathbf{s} + \mathbf{n}_{CRM}. \tag{9}$$

with the elements of the $\mathbf{A}_{CRM}$ matrix being:

$$a_{CRM_{i,j}} = (a_{i,j} - a_{M,j}), \qquad i = 1...M-1, \quad j = 1...N \tag{10}$$

The equation (9) can be rewritten in terms of the original mixtures as follows:

$$\tilde{\mathbf{x}}_{CRM} = \mathbf{T}_{CRM}(\mathbf{A}\mathbf{s} + \mathbf{n}). \tag{11}$$

where $\mathbf{T}_{CRM} \in \Re^{M-1 \times M}$, is a linear transformation applied to the real unknown mixing matrix $\mathbf{A}$. The linear transformation $\mathbf{T}_{CRM}$ is given by:

$$\mathbf{T}_{CRM} = \begin{bmatrix} 1 & 0 & \dots & 0 & -1 \\ 0 & 1 & \dots & 0 & -1 \\ \vdots & \vdots & \dots & \vdots & -1 \\ 0 & 0 & \dots & 1 & -1 \end{bmatrix}.$$

This transform implies a loss in the number of measures: if one has M electrodes placed on the head surface, the CRM montage will only have $M-1$ measures. Therefore, in order to obtain a solution for the BSS problem, one has to use more sensors than sources ($M > N$). All the simulation results presented in the sequel (section 4.1) respect this condition.

Starting from $\tilde{\mathbf{x}}_{CRM}$, the source separation algorithm will compute a $(N \times M - 1)$ non-singular separation matrix $\mathbf{W}_{CRM}$, which can be used to obtain the transfer matrix $\mathbf{G}_{CRM} = \mathbf{W}_{CRM}\mathbf{A}_{CRM} = \mathbf{W}_{CRM}\mathbf{T}_{CRM}\mathbf{A}$ and to compute the *IS* for the CRM from equations (4) and (5).

Estimating the Noise in CRM. As the noise affects the reference electrode as the others, it will be present in the common referenced signals $\tilde{x}_{CRM,i}$ in (8):

$$n_{CRM,i} = n_i - n_M \tag{12}$$

Considering that all noises are independent zero-mean white Gaussian of standard deviation σ, we can compute the power of $n_{CRM,i}$ as follows:

$$\sigma^2_{CRM} = \sigma^2_i + \sigma^2_M = 2\sigma^2. \tag{13}$$

that is, the noise affecting the CRM measures is twice as powerful as for the ideal zero-referenced montage. Consequently, even if all sources are found by source separation, the performance index *IS* should be worse.

3.2. Augmented Average Reference Montage (AARM)

As mentioned above, the Average Reference Montage is obtained from the previously described CRM. More precisely, the mixed signals of the ARM can be derived from the CRM as follows:

$$\tilde{x}_{ARM,i} = \tilde{x}_{CRM,i} - \tilde{R}_{avg}, \quad \text{with} \quad \tilde{R}_{avg} = \frac{1}{M-1} \sum_{i=1}^{M-1} \tilde{x}_{CRM,i} \tag{14}$$

As our goal is to estimate the *IS*, we must write the newly obtained average-referenced measures as a mixture of the original sources $\mathbf{s}$. Writing (14) in terms of its hypothetical zero-referenced real potentials and noise vectors, the last zero-referenced potential $\tilde{x}_M$ disappear and we obtain:

$$\tilde{x}_{ARM,i} = x_i - \frac{1}{M-1} \sum_{j=1}^{M-1} x_j + n_i - \frac{1}{M-1} \sum_{j=1}^{M-1} n_j = x_{ARM,i} + n_{ARM,i}. \tag{15}$$

Now, it is possible to write the new BSS model for the average reference montage as follows:

$$\tilde{\mathbf{x}}_{ARM} = \mathbf{A}_{ARM}\mathbf{s} + \mathbf{n}_{ARM}. \tag{16}$$

with

$$a_{ARM_{i,j}} = (a_{i,j} - a_{M,j}) - \frac{1}{M-1} \sum_{j=1}^{M-1} (a_{i,j} - a_{M,j}), \qquad i = 1 \ldots M-1 \tag{17}$$

However, the $\mathbf{A}_{ARM}$ matrix (17) is singular, so any BSS algorithm fails in finding all the sources. From another point of view, the singularity of the mixing matrix enlightens the fact that by removing the mean signal we lose some information. In order to avoid this lost of information one can add the average reference as an extra virtual signal in the average reference montage. Consequently, one can obtain an augmented ARM (AARM) having M measures by adding a last measure to the ARM montage. For purposes of following the same logic in the equations we obtain this last measure $-\tilde{R}_{Avg}$

as a linear combination of the ideal zero-referenced potentials:

$$\tilde{x}_{AARM,M} = x_M - \frac{1}{M-1}\sum_{j=1}^{M-1} x_j + n_M - \frac{1}{M-1}\sum_{j=1}^{M-1} n_j = x_{AARM,M} + n_{AARM,M} \tag{18}$$

In matrix form, the augmented measures vector $\tilde{\mathbf{x}}_{AARM}$ can be obtained as the noisy mixture of the original sources as follows:

$$\tilde{\mathbf{x}}_{AARM} = \mathbf{A}_{AARM}\mathbf{s} + \mathbf{n}_{AARM} \tag{19}$$

with $\mathbf{A}_{AARM}$, a full-column matrix. The elements of the rows $1, 2, \dots M-1$ of $\mathbf{A}_{AARM}$ are:

$$a_{AARM_{i,j}} = (a_{i,j} - a_{M,j}) - \frac{1}{M-1}\sum_{j=1}^{M-1}(a_{i,j} - a_{M,j}). \tag{20}$$

and those of the last row M:

$$a_{AARM_{M,j}} = -\frac{1}{M-1}\sum_{j=1}^{M-1}(a_{i,j} - a_{M,j})$$

In a compact matrix representation, the equation (20) writes as a linear transformation applied to $\mathbf{A}_{CRM}$ or to $\mathbf{A}$ as follows:

$$\tilde{\mathbf{x}}_{AARM} = \mathbf{T}_{AARM}(\mathbf{A}_{CRM}\mathbf{s} + \mathbf{n}_{CRM}) = \mathbf{T}_{AARM}\mathbf{T}_{CRM}(\mathbf{A}\mathbf{s} + \mathbf{n}) \tag{21}$$

where $\mathbf{T}_{AARM} \in \Re^{M \times M-1}$, is the linear transformation applied to $\mathbf{A}_R$:

$$\mathbf{T}_{AARM} = \begin{bmatrix} 1-\frac{1}{M-1} & -\frac{1}{M-1} & \cdots & -\frac{1}{M-1} \\ -\frac{1}{M-1} & 1-\frac{1}{M-1} & \ddots & \vdots \\ \vdots & \ddots & \ddots & -\frac{1}{M-1} \\ -\frac{1}{M-1} & \cdots & -\frac{1}{M-1} & 1-\frac{1}{M-1} \\ -\frac{1}{M-1} & -\frac{1}{M-1} & -\frac{1}{M-1} & -\frac{1}{M-1} \end{bmatrix}$$

Thus, the obtained mixture is redundant (or, equivalently, the $\mathbf{A}_{AARM}$ matrix is singular) and a step estimating the number of sources (AIC, MDL, BIC – see above) must be included in the BSS algorithms. In this paper, the effectiveness of source number evaluation by these criteria is not tested, as again, the objective is to evaluate the different montages and not source separation methods. Therefore, we have used only the MDL criterion. Consequently (remember that $M > M-1 \geq N$), the BSS algorithms return a separation matrix $\mathbf{W}_{AARM}$ ($N \times M$) and the complete transfer matrix $\mathbf{G}_{AARM} = \mathbf{W}_{AARM}\mathbf{A}_{AARM} = \mathbf{W}_{AARM}\mathbf{T}_{AARM}\mathbf{T}_{CRM}\mathbf{A}$ is square ($N \times N$), and therefore the separability index can again be computed according to (4) and (5).

Estimating the Noise in AARM. The noise analysis is performed using the same approach as for the CRM. From (15) and (18), we have:

$$n_{AARM,i} = n_i - \frac{1}{M-1}\sum_{j=1}^{M-1} n_j, \qquad i = 1...M-1 \tag{22}$$

with

$$n_{AARM,M} = n_M - \frac{1}{M-1}\sum_{j=1}^{M-1} n_j$$

From (22), considering that all noise vectors in $\tilde{\mathbf{x}}_{AARM}$ are zero-mean white Gaussian independent noises of standard deviation σ, we can compute the power of $n_{AARM,i}$ as follows:

$$\begin{aligned} \sigma^2_{AARM,i} &= \mathbb{E}[(n_{AARM,i})^2] = \tfrac{M-2}{M-1}\sigma^2, \qquad i = 1...M-1 \\ \sigma^2_{AARM,M} &= \mathbb{E}[(n_{AARM,M})^2] = \tfrac{M}{M-1}\sigma^2 \end{aligned} \tag{23}$$

where $\mathbb{E}[\cdot]$ is the expected value operator.

3.3. Augmented Bipolar Longitudinal Montage (ABLM)

As ARM, bipolar montages can be obtained also from the CRM EEG recordings as follows:

$$\tilde{x}_{BLM,i} = \tilde{x}_{CRM,i} - \tilde{x}_{CRM,j} \tag{24}$$

with i and j corresponding to two neighboring sensors. Considering the $(M-1)$ CRM measures, only $(M-2)$ BLM independent measures can be obtained, so the system will be under-determined and the BSS solution will be incomplete. To simplify the notation and without loss of generality, we consider here the $(M-2)$ measures as being obtained from (24) with $j = i+1$.

To avoid the indetermination, a $(M-1)$-th measure can be introduced in the model to form the augmented BLM as

$$\tilde{x}_{BLM,M-1} = \tilde{x}_{CRM,M-1}$$

i.e., a CRM measure (another solution, without any physiological signification though, would be to close the loop by considering $\tilde{x}_{BLM,M-1} = \tilde{x}_{CRM,M-1} - \tilde{x}_{CRM,1}$). Equation (24) can be written in terms of its hypothetical zero-referenced potentials and noise vectors as follows:

$$\begin{aligned} \tilde{x}_{ABLM,i} &= \tilde{x}_{CRM,i} - \tilde{x}_{CRM,i+1} = x_i - x_{i+1} + n_i - n_{i+1} \\ \tilde{x}_{ABLM,M-1} &= \tilde{x}_{CRM,M-1} = x_{M-1} - x_M + n_{M-1} - n_M \end{aligned} \tag{25}$$

In matrix form, the ABLM montage writes as follows:

$$\tilde{\mathbf{x}}_{ABLM} = \mathbf{A}_{ABLM}\mathbf{s} + \mathbf{n}_{ABLM} \tag{26}$$

and the elements of rows $i = 1...M-1$ of $\mathbf{A}_{ABLM}$ are:

$$a_{ABLM_{i,j}} = (a_{i,j} - a_{i+1,j}) \tag{27}$$

We can also rewrite equation (26) in a matrix representation as follows:

$$\tilde{\mathbf{x}}_{ABLM} = \mathbf{T}_{ABLM}(\mathbf{A}_{CRM}\mathbf{s} + \mathbf{n}_{CRM}) = \mathbf{T}_{ABLM}\mathbf{T}_{CRM}(\mathbf{A}\mathbf{s} + \mathbf{n}) \qquad (28)$$

where $\mathbf{T}_{ABLM} \in \Re^{(M-1)\times(M-1)}$, is the linear transformation:

$$\mathbf{T}_{ABLM} = \begin{bmatrix} 1 & -1 & 0 & \dots & 0 \\ 0 & 1 & -1 & \ddots & \vdots \\ \vdots & \ddots & \ddots & \ddots & 0 \\ 0 & \dots & 0 & 1 & -1 \\ 0 & 0 & \dots & 0 & 1 \end{bmatrix}$$

The system being full-ranked, BSS algorithms provide a separation matrix $\mathbf{W}_{ABLM}$ $(N \times M-1)$ and the separability index is calculated from the $(N \times N)$ transfer matrix: $\mathbf{G}_{ABLM} = \mathbf{W}_{ABLM}\mathbf{A}_{ABLM} = \mathbf{W}_{ABLM}\mathbf{T}_{ABLM}\mathbf{T}_{CRM}\mathbf{A}$ by equations (4) and (5).

Estimating the Noise in ABLM. According to (25), the noise affecting longitudinal measures is:

$$n_{ABLM,i} = n_i - n_{i+1}. \qquad (29)$$

If we compare (29) with (12) we can see that they are similar, thus the noise power in longitudinal montage can be obtained by (13).

4. Results

4.1. Simulated EEG

To validate the previous analysis, we simulated four different noisy montages: an "ideal" zero-referenced montage ZRM (3), with a mixing matrix $(N + 1 \times N)$, the "realistic" common cephalic reference montage CRM (9)

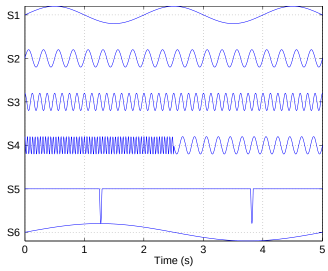

(a) Sources

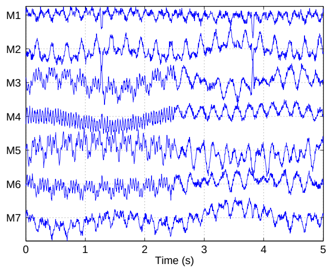

(b) ZRM

Figure 1: Simulated Signals. The ZRM montage is contaminated with Gaussian white noise, SNR=10dB

and the derived augmented average AARM (19) and Augmented Bipolar ABLM (26) montages. We tested three BSS algorithms (SOBI-RO, SOBI, FastICA) in order to separate the mixtures from the different montages and we have taken the *IS* as the performance evaluation criterion.

A set of $N = 6$ signals with different frequencies and shapes with a duration time of 5 s and a sampling rate of 256 Hz was created to be the original zero-referenced source signals (brain frequency range signals and eye artefacts). One thousand simulated noisy EEG recordings were obtained by mixing the sources using random $(N + 1 \times N)$ mixing matrices (uniform distribution between -1 and 1). For each mixture, 5 levels of Gaussian noise were added (SNR = 0, 5, 10, 15 and 20 dB). Then, with the obtained $N + 1$ mixed signals (ZRM EEG simulated potentials) we proceeded to implement the three montages mentioned before (CRM, AARM, ABLM). An example of sources and simulated EEG is presented in Fig. 1 and Fig. 2).

Table 1 presents the average over 1000 different simulations for the 5 different SNR values for each one of the three BSS algorithms. According

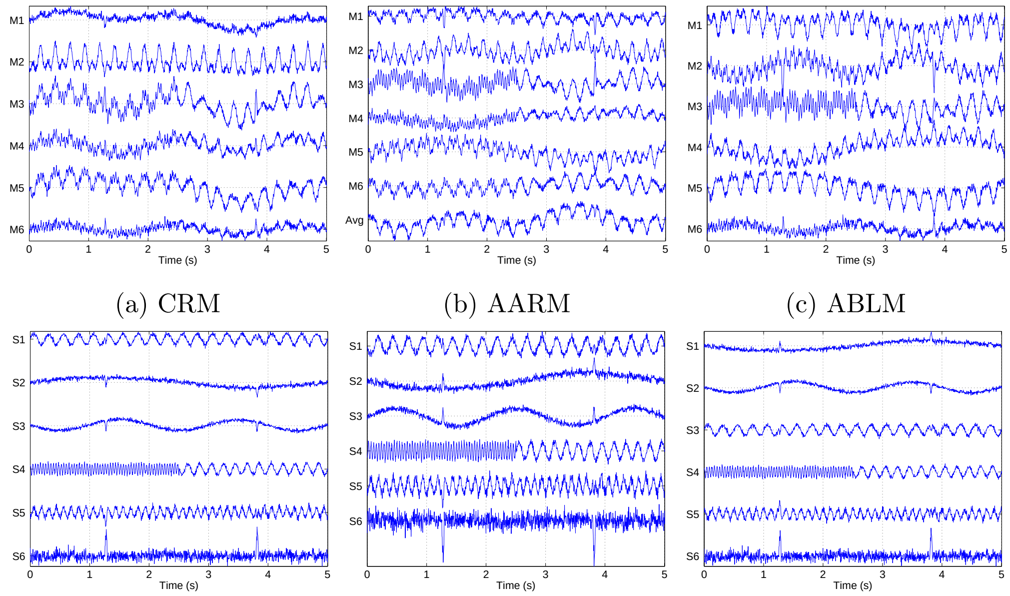

(a) CRM (b) AARM (c) ABLM

(d) BSS for CRM (e) BSS for AARM (f) BSS for ABLM

Figure 2: Simulated noisy (white Gaussian) montages and estimated sources, SNR = 10dB

to the noise evaluation from (13) and (23), the separation results should be different.

As expected, the ideal Zero-Reference Montage presents the best performances, but this ideal condition cannot be obtained in practice and should be seen as an asymptotic best possible value.

Among the possible realistic montages, the AARM has obtained the best IS indices for all the BSS algorithms used in this test, as the noise that affects it is smaller than for CRM and for ABLM. Moreover, as seen in (22), when the number of sensors M increases, the average montage noise tends towards the ZRM noise. The other two classical montages (CRM and ABLM) are noisier and therefore the obtained results are less accurate. Another important observation is that SOBI-RO performs better than the other algorithms, as remarked also in [9, 17].

4.2. Real EEG Signals

The previous simulation needs to be validated on real signals. Real long-time EEG signals ($\approx$ 10 minutes) were recorded using 24 measuring electrodes, placed on the scalp according to the international 10-20 system (Fig. 3) with a 25-th electrode, placed near the eyes in FPz, used as cephalic common reference. The recorded signals were sampled at 256 and notch filtered at 50 Hz. The ECG was also routinely recorded in the same time. Ten different EEGs recorded using the classical common reference montage CRM were selected from our data base, all with an ECG artefact visually identified by the medical experts. For each of the selected EEGs, we considered 10 windows having a duration of 20 seconds each, in order to have a sufficient number of samples and thus a reliable source separation result. The other

BSS Algorithms	Signal to Noise Ratio (SNR,dB)				
	0	5	10	15	20
	Zero Reference Montage (ZRM)				
SOBI-RO	0.09059	0.0511	0.02762	0.01575	0.01162
SOBI	0.14554	0.10598	0.07216	0.0452	0.02552
FastICA	0.19104	0.11332	0.0748	0.05225	0.03941
	Common Reference Montage (CRM)				
SOBI-RO	0.13836	0.09701	0.062	0.03693	0.02578
SOBI	0.17445	0.14395	0.11377	0.08633	0.06104
FastICA	0.22403	0.14984	0.1096	0.08085	0.06111
	Average Reference Montage (AARM)				
SOBI-RO	0.11873	0.08333	0.05308	0.03169	0.02209
SOBI	0.14938	0.12342	0.09754	0.07397	0.05239
FastICA	0.19223	0.12848	0.09329	0.06962	0.05253
	Augmented Bipolar Longitudinal Montage (ABLM)				
SOBI-RO	0.14066	0.09728	0.03694	0.03694	0.02573
SOBI	0.17438	0.14399	0.11383	0.08639	0.06117
FastICA	0.22715	0.15026	0.10853	0.08118	0.06148

Table 1: Performance Evaluation *IS*

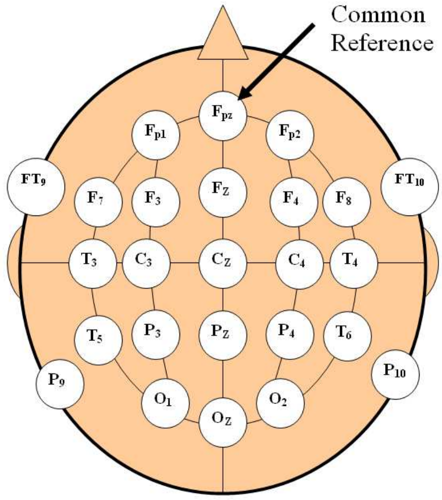

(a)

Figure 3: 10-20 System.

two montages (AARM and ABLM) were derived from the CRM by their respective linear transformations and the three BSS algorithms were applied to recover the sources.

To objectively evaluate the source separation quality, we have estimated the correlation coefficient (6) between the measured known model source s_{ECG} and the estimated source $\hat{s}_{ECG}$. The time lag used to find the maximum correlation between the known ECG signal and the estimated ECG source was within an interval of ± 0.3906 seconds (± 100 samples). The estimated ECG source $\hat{s}_{ECG}$ was identified automatically as the source with the highest correlation coefficient with the measured ECG s_{ECG} within the mentioned time interval. The identification was confirmed by visual inspection for all sources. The results presented in Table 2 were taken as the average correlation coefficient among the 100 EEG epochs of 20 seconds (10 windows

EEG Montages	BSS Algorithms		
	SOBI-RO	SOBI	FastICA
CRM	0.482566	0.503498	0.570881
AARM	0.477575	0.50742	0.571828
ABLM	0.477472	0.505469	0.571005

Table 2: Performance Evaluation $\mathbf{r}_{(s_k,\hat{s}_k)}$.

for each of the 10 long-time recordings).

The obtained results generally confirm that the Average Reference Montage has a positive influence in BSS and it leads to a better separation quality, although the differences are less important than for the simulated signals.

An important difference between simulations and real EEGs is that, according to the proposed criterion, the order of the algorithms changes: FastICA is globally better than SOBI and SOBI-RO, which gives finally the worse performances. Moreover, in the SOBI-RO case, the order of the montages changes and the CRM seems to give the best separation results. This could be explained, paradoxically, by the robust whitening implemented in SOBI-RO. Indeed this procedure eliminates the influence of the white noise on the estimations of the whitening matrix, *if* the noise is white and independent. On the contrary, if the noise does not respect these conditions, the robust whitening might slightly degrade the estimations of the correlation matrix that intervenes in the whitening. SOBI algorithm, identical to SOBI-RO except for the whitening, performs in this case better.

Another situation is encountered for FastICA. In fact, FastICA was the algorithm who obtained the highest correlation coefficient for the estimated

ECG signal. As we mentioned before the ICA algorithms favor the extraction of non Gaussian sources. Moreover, FastICA uses a deflation procedure that extracts first (and with better quality) the sources having the highest kurtosis, *i.e.*, the peaky non-stationary signals like the ECG and the eye-blinking artefacts.

To conclude, SOBI and FastICA algorithms obtain the best performances using the AARM, while this montage leads to the second performance for the SOBI-RO.

An example of source separation for the three montages (CRM, AARM and ABLM) is presented in Fig. 4 (the figured signals are zoomed to a time interval of 5 seconds for easier interpretation, also the estimated sources for the three montages were re-arranged in the same order to ease the visual inspection). Apparently all estimations looks very similar, however remarkable differences can be appreciated (in red) in figures 4d) and 4f). Taking into account the previous results it is possible that real sources looks more like the sources esimated with the AARM (figure 4e).

5. Conclusion

The main goal of this communication is to analyse the most employed EEG montages from a source separation point of view. We have shown in a Monte Carlo Simulation that in noisy conditions, the best results are obtained by using the Average Referenced Montage (ARM), augmented with the computed average measure (AARM) who tends asymptotically to the best possible solution (Zero Referenced ZRM). The simulation results are generally confirmed on real scalp EEGs, both by visual analysis and by a

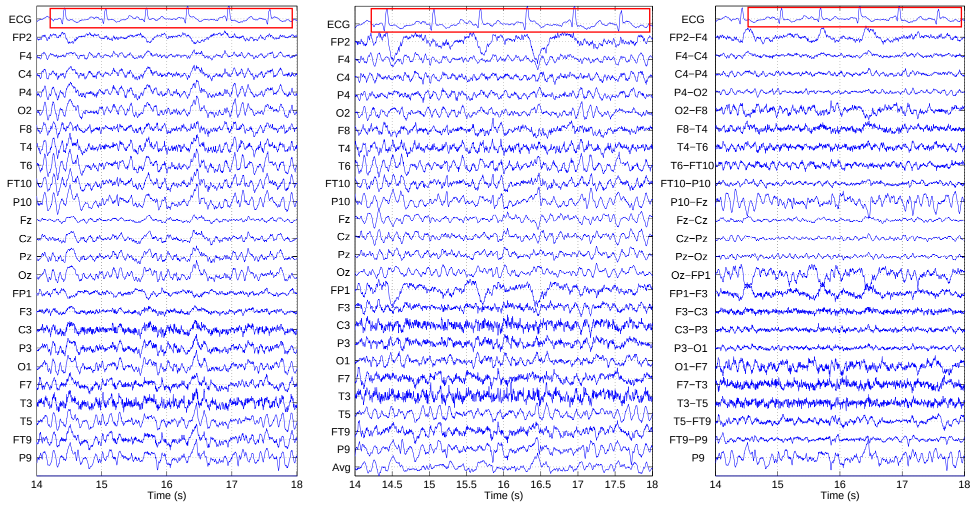

(a) CRM. (b) AARM. (c) ABLM.

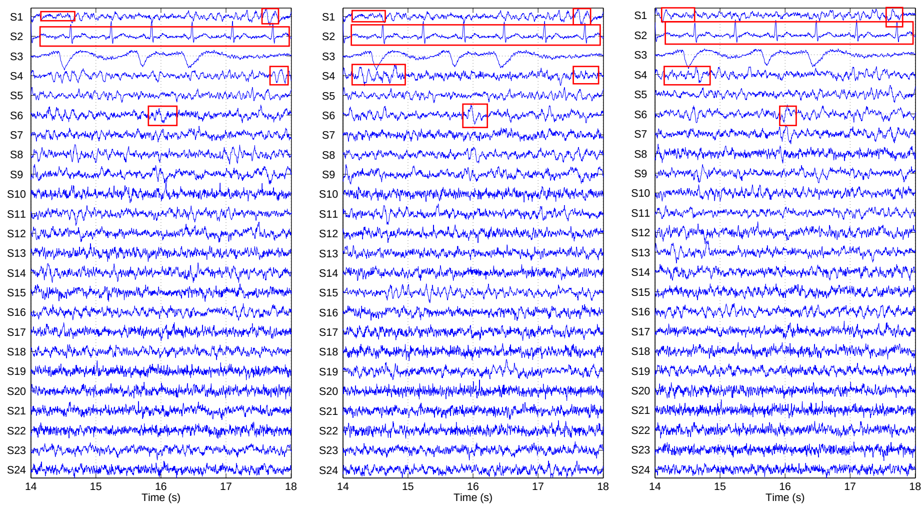

(d) BSS for CRM. (e) BSS for AARM. (f) BSS for ABLM.

Figure 4: Real EEG montages and estimated sources (FastICA).

newly introduced performance criterion, based on the similarity between one of the estimated sources and a simultaneously recorded known signal. In particular the ECG or, possibly, the ocular artefacts can be measured simultaneously by an Electrocardiogram or an Electro-oculogram respectively and thus they can be used to implement the proposed cross-correlation criterion.

The presented analysis is based on the assumptions we have made on the noise, considered independent for each electrode including the reference. The results we obtained confirm indirectly this hypothesis: the predicted best montage (AARM) leads to better performances, independent of the source separation algorithm.

Still, the numeric values obtained for the performance criteria depend, both on simulated and real signals, on the employed source separation algorithm. In particular, as for the real signals we use the ECG signal as a comparison term, using algorithms that furnish the best estimation for the ECG source leads to better performances. This is the case of FastICA, the only tested algorithm based on high order statistics, and known to privilege peaky sources (high kurtosis) like the ECG. In other words, based on the presented results, one cannot conclude that FastICA better separate real EEG signals, although it better estimates the ECG artefact. The problem of performing an evaluation of the quality of sources in real signals remains open.

An interesting point, currently under analysis, is the non-cephalic reference acquisition system analysis. This approach will be presented and compared to the cephalic recording system in a future work.

[1] J. Dien, Issues in the application of the average reference: review, cri-

tiques and recommendations, Behavior Research Methods, Instruments, & Computers 30 (1) (1998) 34–43.

[2] D. Yao, A method to standardize a reference of scalp EEG recordings to a point at infinity, Physiological Measurement 22 (2001) 693–711.

[3] S. Schachter, All about epilepsy & seizures, http://www.epilepsy.com/epilepsy/eeg_read (2008).

[4] B. Fisch, S. R., Fisch and Spehlmann's EEG Primer: Basic Principles of Digital Analog EEG, Elsevier Health Sciences, 1999.

[5] R. Croft, R. Barrey, Removal of ocular artifact from the eeg: a review, Neurophysiologie Clinique/Clinical Neurophysiology 30 (1) (2000) 5–19.

[6] A. Delorme, S. Makeig, T. Sejnowski, Automatic artifact rejection for eeg data using high-order statistics and independent component analysis (2001).

[7] C. James, O. Gibson, Temporally constrained ICA: an application to artifact rejection in electromagnetic brain signal analysis, IEEE Transactions on Biomedical Engineering 50 (9) (2003) 1108–1116.

[8] K. Ting, P. Fung, C. Chang, F. Chan, Automatic correction of artifact from single-trial event-related potentials by blind source separation using second order statistics only, Medical Engineering and Physics 28 (8) (2006) 780–794.

[9] R. Romo-Vázquez, R. Ranta, V. Louis-Dorr, D. Maquin, EEG ocular artefacts and noise removal, in: 29th Annual International Conference

of the IEEE Engineering in Medicine and Biology Society, EMBC'07, 2007.

[10] S. Hu, M. Stead, G. Worrel, Automatic identification and removal of scalp reference signal for intracranial EEGs based on Independent Component Analysis, IEEE Trans. Biomed. Eng. 54 (9) (2007) 1560–1572.

[11] A. Cichocki, S. Amari, Adaptive Blind Signal and Image Processing Learning Algorithms and Applications, John Wiley & Sons, New York, USA, 2002.

[12] A. Hyvärinen, E. Oja, A fast fixed-point algorithm for independent component analysis, Neural Computation 9 (7) (1997) 1483–1492.

[13] A. Belouchrani, K. Abed-Meriam, C. J., M. E., A blind source separation technique using second order statistics, IEEE Transactions on Signal Processing 45 (2) (1997) 434–444.

[14] A. Belouchrani, A. Cichocki, Robust withening procedure in blind source separation context, Electronic Letters 36 (24) (2000) 2050–2051.

[15] J. Kierkels, G. van Boxtel, L. Vogten, A model-based objective evaluation of eye movement correction in EEG recordings, IEEE Transactions on Biomedical Engineering 53 (2) (2006) 246–253.

[16] S. Romero, M. A. Mañanas, M. J. Barbanoj, A comparative study of automatic techniques for ocular artifact reduction in spontaneous eeg signals based on clinical target variables: A simulation case, Computers in biology and medicine 38 (3) (2008) 348–360.

[17] R. Salido-Ruiz, R. Romo-Vazquez, R. Ranta, L. Leija, Analysis of 5 source separation algorithms on simulated EEG signals, Research in Computer Science / Special Issue in Electronics and Biomedical Informatics, Computer Science and Informatics 35 (2008) 177–186.